A Scoping Review on Stoichiometry of CCTO with Doping Process for Improvement of Dielectric Resonator Antenna

Hasanah Safein Shafie[2,*a)], Julie Juliewatty Mohamed[1*], Ira Fazlin Mohd Fauzi[2], Md Fadzil Ain[3], Nor Fadzilah Mohamed[1], Mohamed Johari Abu[1],

[1] *Faculty of Bioengineering And Technology (FBKT), Universiti Malaysia Kelantan (UMK), Jeli Campus, 02600 Jeli, Kelantan, Malaysia*
[2] *Department of Mathemetics Science And Computer (JMSK), Politeknik Kota Bharu, 16450 Ketereh, Kelantan, Malaysia*
[3] *School of Electrical and Electronic Engineering, Universiti Sains Malaysia, Kampus Kejuruteraan 14300 Nibong Tebal Pulau Pinang, Malaysia*

Author Email:
[a)] hasanah@pkb.edu.my

Received 15 October 2024, Accepted 5 December 2024, Published on 4 March 2025

Abstract: The small size and great efficiency of Dielectric Resonator Antennas (DRAs) make them essential parts of contemporary wireless communication systems. A viable contender for DRA applications, calcium copper titanate (CCTO) is a perovskite-type ceramic material that has attracted a lot of attention because of its high dielectric constant and low loss properties. The stoichiometric composition of CCTO, especially when altered by doping procedures, has a significant impact on its dielectric characteristics. This scoping study methodically examines how different doping elements affect the CCTO stoichiometry and how that affects the DRAs' dielectric characteristics. To improve the electrical, mechanical, and thermal characteristics of CCTO, doping methods including rare-earth metals, transition metals, and alkaline-earth metals are frequently employed. We examine a wide range of research on this topic. The structural integrity, permittivity, loss tangent, and resonance properties of CCTO—all essential for maximizing DRA performance—are examined in relation to these doping factors. There is further discussion of how processing parameters, sintering temperature, and dopant concentration affect the overall behavior of the material. Important results show that CCTO is more appropriate for high-frequency DRA applications when selective doping is used to greatly increase the dielectric constant, reduce the loss tangent, and improve frequency tunability. Better temperature stability, which is essential for reliable operation in real-world wireless systems, is another benefit of doping with certain elements. Additionally, the study points up knowledge gaps on the connection between dopant concentration and DRA performance, especially in reference to the interaction between dielectric resonance and material stoichiometry. In Conclusion, this study emphasizes how crucial it is to optimize the doping procedure in order to fine-tune the CCTO stoichiometry for better DRA performance. Investigations into new dopants, their mechanisms in the CCTO matrix, and the scalability of doping methods for commercial DRA applications should be the main goals of future studies.
Keywords: stoichiometry dielectric, resonator, antenna, enhancement

INTRODUCTION

In recent years, the pursuit of advanced materials for electronic applications has propelled the exploration and development of innovative dielectric materials. Among these, Calcium Copper Titanate (CCTO), a perovskite-based ceramic compound, has emerged as a promising candidate due to its intriguing dielectric properties [1]–[3]. However, its inherent limitations, such as high dielectric loss and low dielectric constant at room

temperature, have prompted researchers to delve into modification strategies to enhance its performance. This scoping review aims to comprehensively analyze the impact of stoichiometry modification via doping processes on the dielectric properties of CCTOv[4].

CCTO, known for its high permittivity and potential applications in capacitors, sensors, and electronic devices, presents challenges related to its insufficient dielectric characteristics for practical utilization. The process of doping, involving the controlled introduction of foreign elements into the CCTO lattice, has emerged as a prominent avenue to alter its stoichiometry, structure, and ultimately, dielectric behavior [5]. Through this scoping review, we aim to provide a holistic understanding of the diverse doping techniques employed, exploring their efficacy in tailoring the stoichiometry and improving the dielectric response of CCTO [6].

This review will extensively survey and synthesize the existing literature, encompassing research articles, patents, and conference proceedings, to map the landscape of CCTO doping methodologies. It will delve into the diverse types of dopants utilized, their concentrations, synthesis methods, and their consequent impacts on the dielectric properties of CCTO. By elucidating the underlying mechanisms and effects of doping on CCTO, this review endeavors to offer valuable insights into optimizing the stoichiometric composition of CCTO for enhanced dielectric performance [7]–[9].

Furthermore, this scoping review seeks to identify research gaps, challenges, and opportunities within the realm of CCTO doping strategies. It aims to facilitate the development of new approaches and directions for researchers and practitioners aiming to advance the dielectric properties of CCTO, paving the way for its wider application in various electronic and technological domains [10].

These criteria help streamline the search process and ensure that the literature selected for analysis aligns closely with the research objectives.

TABLE 1 The search string.

Scopus	TITLE-ABS-KEY ((enhancement OR improvement) AND of AND (dielectric OR semiconductor) AND resonator AND (antenna OR rectangular OR dra) (enhancement OR improvement) AND of AND (dielectric OR semiconductor) AND resonator AND (antenna OR rectangular)) AND (LIMIT-TO (DOCTYPE , "ar") OR LIMIT-TO (DOCTYPE , "cp") OR LIMIT-TO (DOCTYPE , "re")) AND (LIMIT-TO (PUBYEAR , 2013) OR LIMIT-TO (PUBYEAR , 2014) OR LIMIT-TO (PUBYEAR , 2015) OR LIMIT-TO (PUBYEAR , 2016) OR LIMIT-TO (PUBYEAR , 2017) OR LIMIT-TO (PUBYEAR , 2018) OR LIMIT-TO (PUBYEAR , 2019) OR LIMIT-TO (PUBYEAR , 2020) OR LIMIT-TO (PUBYEAR , 2021) OR LIMIT-TO (PUBYEAR , 2022) OR LIMIT-TO (PUBYEAR , 2023))

TABLE 2 The selection criterion is searching

Criterion	**Inclusion**	**Exclusion**
Language	English	Non-English
Time line	2013 – 2023	< 2013
Literature type	Journal (Article), Conference	Book, Review
Publication Stage	Final	In Press

The search string

scoping	keyword	Title abs key

Scopus	Scope 1	TITLE-ABS-KEY (performance AND (stoichiometry OR calculation) AND type AND of AND doping AND dielectric AND effect)
	Scope 2	TITLE-ABS-KEY (type AND of AND (doping OR galium) AND dielectric AND effect AND ccto)
		TITLE-ABS-KEY ((impact OR performance) AND stoichiometry AND doping AND (dielectric OR communication OR antenna))
	Scope 3	

REVIEW OF STUDY

Scope 1: type of dopping

The improved dielectric properties and voltage-current nonlinearity of nickel-doped CaCu3Ti4O12 (CCNTO) ceramics prepared by solid-state reaction were investigated. The approach of A′-site Ni doping resulted in improved dielectric properties in the CaCu3Ti4O12 (CCTO) system, with a dielectric constant ε′≈1.51×105 and dielectric loss tanδ≈0.051 found for the sample with a Ni doping of 20% (CCNTO20) at room temperature and 1 kHz. The X-ray photoelectron spectroscopy (XPS) analysis of the CCTO and the specimen with a Ni doping of 25% (CCNTO25) verified the co-existence of Cu+/Cu2+ and Ti3+/Ti4+. A steady increase in ε′(f) and a slight increase in α observed upon initial Ni doping were ascribed to a more Cu-rich phase in the intergranular phase caused by the Ni substitution in the grains. The low-frequency relaxation leading to a distinct enhancement in ε′(f) beginning with CCNTO25 was confirmed to be a Maxwell-Wagner-type relaxation strongly affected by the Ni-related phase with the formation of a core-shell structure. The decrease of the dielectric loss was associated with the promoted densification of CCNTO and the increase of Cu vacancies, due to Ni doping on the Cu sites. In addition, the Ni dopant had a certain effect on tuning the current-voltage characteristics of the CCTO ceramics. The present A′-site Ni doping experiments demonstrate the extrinsic effect underlying the giant dielectric constant and provides a promising approach for developing practical applications [11].

The influence of NiO-doping on the microstructure and dielectric properties of CaCu3Ti4O12-xNiO (x=0, 0.003, 0.006, 0.010, 0.015, and 0.020) ceramics has been investigated using SEM, Raman spectra and dielectric spectrum measurements. The positron annihilation lifetime spectra (PALS) are used to investigate the influence of defects on the dielectric properties. The SEM results show that the grain morphology varies significantly with increasing NiO content. An appropriate small amount of NiO can promote the grain growth, which is beneficial to improve the dielectric properties in a CaCu3Ti4O12 (CCTO) system. Positron results show that there are vacancy-type defects in the experimental samples, and the concentration of the defect and the defect type both change with increasing NiO content. The effects of microstructure including the grain morphology and the vacancy defects on the mechanism of the dielectric properties by adding NiO are discussed. The results demonstrate the importance of the grain morphology and the characteristic of defects in controlling the electrical properties of CCTO ceramics[12].

In this study, ceramic CaCu3 Ti4 O12 (CCTO) and CaCu3−x Mgx Ti4 O12 solid solutions in which $0.1 \leq x \leq 0.5$ were prepared by the mechanochemical method, realized by a high-energy ball milling technique. The effects of the Mg2+ ion concentration and sintering time on the dielectric response in the prepared ceramics were investigated and discussed. It was demonstrated that, by the use of a sufficiently high energy of mechanochemical treatment, it is possible to produce a crystalline product after only 2 h of milling the mixture of the oxide substrates. Both the addition of magnesium ions and the longer sintering time of the mechanochemically-produced ceramics cause excessive grain growth and significantly affect the dielectric properties of the materials. The X-ray diffraction (XRD) analysis showed that all of the as-prepared solid

solutions, CaCu3−x Mgx Ti4 O12 ($0.0 \leq x \leq 0.5$), regardless of the sintering time, exhibit a cubic perovskite single phase. The dielectric study showed two major contributions associated with the grains and the grain boundaries. The analysis of the electric modules of these ceramics confirmed the occurrence of Maxwell–Wagner type relaxation, which is dependent on the temperature [13]

By using a traditional solid state reaction, CaCu3Ti4-xCoxO12 (x = 0, 0.2, 0.4) ceramics were created, and the effects of cobalt doping on their room temperature magnetic and dielectric properties were examined. Energy dispersive X-ray spectroscopy and X-ray diffraction both verified the existence of Cu and Co rich phases at the grain boundaries of Co-doped ceramics. In pure CaCu3Ti4O12 (CCTO), scanning electron microscopy micrographs of co-doped samples revealed a remarkable transition from regular polyhedral particle type to sheet-like grains with specific growth orientation. The enormous dielectric constant of undoped CaCu3Ti4O12 across a wide temperature and frequency range is well known. While the second relaxation process was clearly separated in the low frequency region at 5 at. % and 10 at. % Co doping, the dielectric constant value was only slightly altered.[14]

Ceramic samples of CaCu3(Ti1-xHfx)4O12(CCTHO) were prepared by solid state reaction method. The influences of Hf+4 ions substitution on the structural, optical and dielectric properties of the prepared samples were investigated using X-ray diffraction, diffuse reflectance spectroscopy and impedance spectroscopy respectively. The solubility limit of Hf in CaCu3Ti4O12 (CCTO) is found to be ~ 2%. The optical spectroscopy data reveals that with Hf doping the optical band gap increases. Further we observed that with Hf substitution in CCTO at Ti site improves the dielectric properties, i.e. the value of dielectric constant (ε′) increases and that of dielectric loss (tanδ) decreases with respect to parent un-doped CCTO sample. Two dielectric relaxations are observed in Hf doped sample, whereas only one relaxation is observed in CCTO. The characteristic dielectric relaxation frequency shifts towards higher values with Hf doping. Further from the fitting of ε′ versus frequency data it appears that the relaxation mechanism shifts from Debye to Cole–Cole type [15]

Ceramics in the solid solution system, Ba0.9Ca0.1Ti0.9Zr0.1O3–xBi3+ (x = 0.000–0.030) were prepared by hydrothermal and were assisted by microwave sintering. Effects of Bi3+ content on the phase transition, microstructure, and electrical properties of ceramics were investigated. The single phase perovskite-type ceramics showed different polymorphs and the grain size was significantly influenced with the doping of Bi3+. Dielectric measurements indicated excellent dielectric relaxation behavior for x = 0.005 and x = 0.030. At x = 0.015 and x = 0.020, samples show giant dielectric constant (near 200,000) and lower dielectric loss (lower than 1.2), compared with other giant permittivity materials such as CCTO. The relationship between TC and 2EC was investigated and a novel conclusion of the 2EC was increased with increasing TC was reached. A maximum value of d33 = 265 pC/N was observed at x = 0.025 for the emergence of TO–T. That is because piezoelectrics always possessed high d33 near morphotropic phase boundary [16].

Compositions based on Ca1−xSrxCu3Ti4O12(x = 0, 0.05, 0.1, 0.2) were prepared via the conventional solid state synthesis methods, influence of semiconductive grain and microstructure on the dielectric properties of CaCu3Ti4O12 ceramics was studied. UV–vis absorption spectra and photoluminescence measurement indicated that the semiconductive of grains changed with Sr2+ doping, and the band gap of materials increased from 2.25 eV to 2.30 eV. According to the model Schottky-type barrier formed between the grain boundaries (GBs), we analyzed that increased band gap would lead to increase of the potential barrier of height, thus grain boundary resistance increased and the dielectric constants decreased. However, microstructure of Ca1−xSrxCu3Ti4O12 contributed to the dielectric properties were researched, the grain size became larger with Sr2+ doping, thus the dielectric constants increased and grain boundary resistance decreased with Sr2+ doping. The results showed that Schottky-type barriers between GBs were the factors to form the special dielectric properties of CCTO, and microstructure would influence the dielectric properties notably [17]

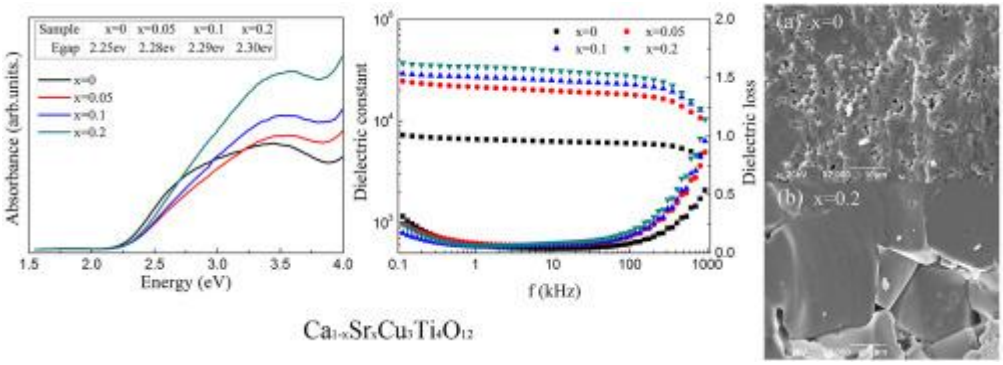

Figure [17].

Using a traditional solid state reaction, CaCu3Ti4-xCoxO12 (x = 0, 0.2, 0.4) ceramics were created, and the effects of cobalt doping on their room temperature magnetic and dielectric characteristics were examined. The presence of Cu and Co rich phases at the grain boundaries of Co-doped ceramics was confirmed by both energy dispersive X-ray spectroscopy and X-ray diffraction. Co-doped samples' scanning electron microscopy micrographs revealed a notable transition from the typical polyhedral particle type found in pure CaCu3Ti4O12 (CCTO) to sheet-like grains with a specific growth direction. The massive dielectric constant of undoped CaCu3Ti4O12 across a wide temperature and frequency range is well known. While the second relaxation process was clearly separated in the low frequency region at 5 at. % and 10 at. % Co doping, the dielectric constant value was only marginally altered. [18].

2.2. **Scope 2: impact of education performance of model/ Effect of Dopping**

The improved dielectric properties and voltage-current nonlinearity of nickel-doped CaCu3Ti4O12 (CCNTO) ceramics prepared by solid-state reaction were investigated. The approach of A′-site Ni doping resulted in improved dielectric properties in the CaCu3Ti4O12 (CCTO) system, with a dielectric constant ε′≈1.51×105 and dielectric loss tanδ≈0.051 found for the sample with a Ni doping of 20% (CCNTO20) at room temperature and 1 kHz. The X-ray photoelectron spectroscopy (XPS) analysis of the CCTO and the specimen with a Ni doping of 25% (CCNTO25) verified the co-existence of Cu+/Cu2+ and Ti3+/Ti4+. A steady increase in ε′(f) and a slight increase in α observed upon initial Ni doping were ascribed to a more Cu-rich phase in the intergranular phase caused by the Ni substitution in the grains. The low-frequency relaxation leading to a distinct enhancement in ε′(f) beginning with CCNTO25 was confirmed to be a Maxwell-Wagner-type relaxation strongly affected by the Ni-related phase with the formation of a core-shell structure. The decrease of the dielectric loss was associated with the promoted densification of CCNTO and the increase of Cu vacancies, due to Ni doping on the Cu sites. In addition, the Ni dopant had a certain effect on tuning the current-voltage characteristics of the CCTO ceramics. The present A′-site Ni doping experiments demonstrate the extrinsic effect underlying the giant dielectric constant and provides a promising approach for developing practical applications [11]

The influence of NiO-doping on the microstructure and dielectric properties of CaCu3Ti4O12-xNiO (x=0, 0.003, 0.006, 0.010, 0.015, and 0.020) ceramics has been investigated using SEM, Raman spectra and dielectric spectrum measurements. The positron annihilation lifetime spectra (PALS) are used to investigate the influence of defects on the dielectric properties. The SEM results show that the grain morphology varies significantly with increasing NiO content. An appropriate small amount of NiO can promote the grain growth, which is beneficial to improve the dielectric properties in a CaCu3Ti4O12 (CCTO) system. Positron results show that there are vacancy-type defects in the experimental samples, and the concentration of the defect and the defect type both change with increasing NiO content. The effects of microstructure including the grain morphology and the vacancy defects on the mechanism of the dielectric properties by adding NiO are discussed. The results demonstrate the importance of the grain morphology and the characteristic of defects in controlling the electrical properties of CCTO ceramics. [12].

In this study, ceramic CaCu3 Ti4 O12 (CCTO) and CaCu3−x Mgx Ti4 O12 solid solutions in which $0.1 \leq x \leq 0.5$ were prepared by the mechanochemical method, realized by a high-energy ball milling technique. The effects of the Mg2+ ion concentration and sintering time on the dielectric response in the prepared ceramics were investigated and discussed. It was demonstrated that, by the use of a sufficiently high energy of

mechanochemical treatment, it is possible to produce a crystalline product after only 2 h of milling the mixture of the oxide substrates. Both the addition of magnesium ions and the longer sintering time of the mechanochemically-produced ceramics cause excessive grain growth and significantly affect the dielectric properties of the materials. The X-ray diffraction (XRD) analysis showed that all of the as-prepared solid solutions, CaCu3−x Mgx Ti4 O12 ($0.0 \leq x \leq 0.5$), regardless of the sintering time, exhibit a cubic perovskite single phase. The dielectric study showed two major contributions associated with the grains and the grain boundaries. The analysis of the electric modules of these ceramics confirmed the occurrence of Maxwell–Wagner type relaxation, which is dependent on the temperature [13].

This study explores the effect of iodine (an anion) substitution on the dielectric and resistive properties of CaCu3Ti4O12-xIx (x = 0, 0.005, 0.05, and 0.20) sintered at 1100 °C for 12 h with the help of impedance and modulus spectroscopy. The electrical measurements were done with varying temperatures (300–450 K) and frequency (20 Hz-1 MHz). The ionic distribution of different ions and iodine and their oxidation states were revealed by EDX and XPS analysis, supporting the synthesis of CCTO ceramics with iodine substitution. The complex plane plots (Z″ vs. Z′ and M″ vs. M′) and spectroscopic plots (Z″ vs. log f and M″ vs. log f) of various compositions at different temperatures suggest that the grains, grain boundaries, and sample-electrode interface contribute to their electrical response and can be represented by a combination of three R–C or R-CPE equivalent circuits. The depressed arcs in the Z″ vs. Z′ plot revealed multiple relaxations with a narrow distribution of time constants. The scaled master plots confirm that the resistive and polarization mechanisms are independent of temperature and are Maxwell-Wagner relaxations type. Broad relaxation peaks and mismatch in peak frequencies of Z″ and M″ vs. log f plots suggest that the relaxation mechanism is dominated by the short-range (localized) movement of charge carriers. The activation energies for grain and grain boundary relaxation processes are ∼0.15 eV and ∼0.2 eV, respectively. Increasing iodine doping from x = 0.005 to x = 0.05 leads to a large increase in the resistance of the specimen, which has been explained based on change of charge compensation for IO• defects from electronic defect e/ to ionic defects VCu// and/or VTi////. The dielectric constant is maximum for the composition, x = 0.2, whereas loss, tan δ is minimum for x = 0.05 [14].

Ceramic samples of CaCu3(Ti1-xHfx)4O12(CCTHO) were prepared by solid state reaction method. The influences of Hf+4 ions substitution on the structural, optical and dielectric properties of the prepared samples were investigated using X-ray diffraction, diffuse reflectance spectroscopy and impedance spectroscopy respectively. The solubility limit of Hf in CaCu3Ti4O12 (CCTO) is found to be ~ 2%. The optical spectroscopy data reveals that with Hf doping the optical band gap increases. Further we observed that with Hf substitution in CCTO at Ti site improves the dielectric properties, i.e. the value of dielectric constant (ε′) increases and that of dielectric loss (tanδ) decreases with respect to parent un-doped CCTO sample. Two dielectric relaxations are observed in Hf doped sample, whereas only one relaxation is observed in CCTO. The characteristic dielectric relaxation frequency shifts towards higher values with Hf doping. Further from the fitting of ε′ versus frequency data it appears that the relaxation mechanism shifts from Debye to Cole–Cole type [15].

Ceramics in the solid solution system, Ba0.9Ca0.1Ti0.9Zr0.1O3–xBi3+ (x = 0.000–0.030) were prepared by hydrothermal and were assisted by microwave sintering. Effects of Bi3+ content on the phase transition, microstructure, and electrical properties of ceramics were investigated. The single phase perovskite-type ceramics showed different polymorphs and the grain size was significantly influenced with the doping of Bi3+. Dielectric measurements indicated excellent dielectric relaxation behavior for x = 0.005 and x = 0.030. At x = 0.015 and x = 0.020, samples show giant dielectric constant (near 200,000) and lower dielectric loss (lower than 1.2), compared with other giant permittivity materials such as CCTO. The relationship between TC and 2EC was investigated and a novel conclusion of the 2EC was increased with increasing TC was reached. A maximum value of d33 = 265 pC/N was observed at x = 0.025 for the emergence of TO–T. That is because piezoelectrics always possessed high d33 near morphotropic phase boundary [16].

Compositions based on Ca1−xSrxCu3Ti4O12(x = 0, 0.05, 0.1, 0.2) were prepared via the conventional solid state synthesis methods, influence of semiconductive grain and microstructure on the dielectric properties of CaCu3Ti4O12 ceramics was studied. UV–vis absorption spectra and photoluminescence measurement indicated that the semiconductive of grains changed with Sr2+ doping, and the band gap of materials increased from 2.25 eV to 2.30 eV. According to the model Schottky-type barrier formed between the grain boundaries (GBs), we analyzed that increased band gap would lead to increase of the potential barrier of height, thus grain boundary resistance increased and the dielectric constants decreased. However, microstructure of

Ca1−xSrxCu3Ti4O12 contributed to the dielectric properties were researched, the grain size became larger with Sr2+ doping, thus the dielectric constants increased and grain boundary resistance decreased with Sr2+ doping. The results showed that Schottky-type barriers between GBs were the factors to form the special dielectric properties of CCTO, and microstructure would influence the dielectric properties notably [17].

CaCu3Ti4-xCoxO12 (x = 0, 0.2, 0.4) ceramics were prepared by a conventional solid state reaction, and the effects of cobalt doping on the room temperature magnetic and dielectric properties were investigated. Both X-ray diffraction and energy dispersive X-ray spectroscopy confirmed the presence of Cu and Co rich phase at grain boundaries of Co-doped ceramics. Scanning electron microscopy micrographs of Co-doped samples showed a striking change from regular polyhedral particle type in pure CaCu3Ti4O12 (CCTO) to sheet-like grains with certain growth orientation. Undoped CaCu3Ti4O12 is well known for its colossal dielectric constant in a broad temperature and frequency range. The dielectric constant value was slightly changed by 5 at. % and 10 at. % Co doping, whereas the second relaxation process was clearly separated in low frequency region at room temperature. A multirelaxation mechanism was proposed to be the origin of the colossal dielectric constant. In addition, the permeability spectra measurements indicated Co-doped CCTO with good magnetic properties, showing the initial permeability (μ′) as high as 5.5 and low magnetic loss (μ″ < 0.2) below 3 MHz. And the interesting ferromagnetic superexchange coupling in Co-doped CaCu3Ti4O12 was discussed [18].

Scope 3: Impact of Health Care –Performance of Popping

Spray-coated crystalline InZnOx-based semiconductors are investigated as a function of [In3+]:[Zn2+] and their performance as TFTs semiconducting channels. More precisely, it is demonstrated that optical, structural, and electron transport properties show a high degree of sensitivity to the films' stoichiometry; that is, the [In3+]:[Zn2+] atomic ratio that equally determines the amorphous or crystalline structure of the film. Yttrium co-doping of InZnOx with [In3+]:[Zn2+] atomic ratio of 6:4 shows that the YInZnOx structure and the key TFT parameters can further be engineered and improved in terms of the on-to-off current modulation ratio and, most importantly, the field effect mobility. It is finally demonstrated that the latter is in excess of 52 cm2 V-1 s-1 by combining crystalline YInZnOx and spray-coated MgO dielectrics. These results identify spray-coated crystalline YInZnOx as a viable TFT semiconducting channel material with respect to enhanced electrical performance and processing requirements in terms of simplicity and cost [19].

The ceramic perovskite solid solutions BaTiO3–BiScO3 (BT–BS) and SrTiO3–Bi(Zn1/2Ti1/2)O3 (ST–BZT) are promising candidates for high-temperature and high-energy density dielectric applications. A-site cation nonstoichiometry was introduced in these two ceramic systems to investigate their effects on the dielectric and transport properties using temperature- and oxygen partial pressure-dependent AC impedance spectroscopy. For p-type BT–BS ceramics, the addition of excess Bi led to effective donor doping along with a significant improvement in insulation properties. A similar effect was observed on introducing Ba vacancies onto the A-sublattice. However, Bi deficiency registered an opposite effect with effective acceptor doping and a deterioration in the bulk resistivity values. For n-type intrinsic ST–BZT ceramics, the addition of excess Sr onto the A-sublattice resulted in a decrease in resistivity values, as expected. Introduction of Sr vacancies or addition of excess Bi on A-site did not appear to affect the insulation properties in air. These results indicate that minor levels of nonstoichiometry can have an important impact on the material properties, and furthermore it demonstrates the difficulties encountered in trying to establish a general model for the defect chemistry of Bi-containing perovskite systems [20].

The impact of antimony (Sb) doping concentration on the different physical properties of transparent conducting tin oxide (SnO2) thin films synthesized through nebulized spray pyrolysis (NSP) method have been explored systematically. X-ray diffraction (XRD) results reveal the tetragonal cassiterite structure of single phase SnO2 and the decrement of crystallite size with rising Sb doping concentration. Uniform and compact surface morphology with continuous distribution of grains and reduction of grain size with increasing dopant amount are illustrated by scanning electron microscopy (SEM). The stoichiometry of SnO2 film with 2% Sb doping is confirmed by energy dispersive X-ray spectroscopy (EDS) study. The optical transmittance is more than 85% in the visible region for undoped film and enhanced in the near infrared (NIR) spectral region for all the films. The transparency is reduced and the optical band gap is found to increase from 3.69 eV to 3.90 eV upon Sb inclusion. The extinction coefficient, refractive index, dielectric constant, dissipation factor, volume energy loss

function, surface energy loss function, optical conductivity and optical density of the films are determined and interpreted for different dopant concentrations. The photoluminescence (PL) spectrum demonstrates the enhancement of emission intensity with increasing Sb incorporation representing its suitability in the application of solid state lighting. The lowest resistivity of 6.435 × 10−4 Ω cm and the highest carrier concentration of 1.316 × 1021 cm−3 are achieved for the film with 8% Sb doping concentration. The mobility of the studied degenerated films is varied from 54.743 cm2/Vs for undoped films to 7.378 cm2/Vs for 8% Sb doped film and limited by ionized impurity scattering. The film deposited with 2% Sb doping level exhibits the highest figure of merit values in both visible and NIR wavelength region indicating its better role in optoelectronic applications [21].

In recent years, silica films have emerged as a novel class of two-dimensional (2D) materials. Several groups succeeded in epitaxial growth of ultrathin SiO2 layers using different growth methods and various substrates. The structures consist of tetrahedral [SiO4] building blocks in two mirror symmetrical planes, connected via oxygen bridges. This arrangement is called a silica bilayer as it is the thinnest 2D arrangement with the stoichiometry SiO2 known today. With all bonds saturated within the nano-sheet, the interaction with the substrate is based on van der Waals forces. Complex ring networks are observed, including hexagonal honeycomb lattices, point defects and domain boundaries, as well as amorphous domains. The network structures are highly tuneable through variation of the substrate, deposition parameters, cooling procedure, introducing dopants or intercalating small species. The amorphous networks and structural defects were resolved with atomic resolution microscopy and modeled with density functional theory and molecular dynamics. Such data contribute to our understanding of the formation and characteristic motifs of glassy systems. Growth studies and doping with other chemical elements reveal ways to tune ring sizes and defects as well as chemical reactivities. The pristine films have been utilized as molecular sieves and for confining molecules in nanocatalysis. Post growth hydroxylation can be used to tweak the reactivity as well. The electronic properties of silica bilayers are favourable for using silica as insulators in 2D material stacks. Due to the fully saturated atomic structure, the bilayer interacts weakly with the substrate and can be described as quasi-freestanding. Recently, a mm-scale film transfer under structure retention has been demonstrated. The chemical and mechanical stability of silica bilayers is very promising for technological applications in 2D heterostacks. Due to the impact of this bilayer system for glass science, catalysis and the field of 2D materials, a large number of theoretical and experimental studies on silica bilayers have been reported in the last years. This review aims to provide an overview on the insights gained on this material and to point out opportunities for further discovery in various fields [22].

Water management in a PEM fuel cell significantly affects the fuel cell performance and durability. The gas diffusion layer (GDL) of a PEM fuel cell plays a critical role in the water management process. In this short communication, we report a simple method to measure the water transport rate across the GDL. Water rejection rates across a GDL at different cathode air-flow rates were measured. Based on the measurement results, the fuel cell operating conditions, such as current density, temperature, air stoichiometry and relative humidity, corresponding to membrane drying and flooding conditions were identified for the particular GDL used. This method can help researchers develop GDLs for a particular fuel cell design with specific operating conditions and optimize the operation conditions for the given PEM fuel cell components [23].

A group of 0.65(Bi0.5Na0.5)TiO3 -0.35(Sr0.7+x + Bi0.2)TiO3 (BNT-S0.7+xBT) composite ceramic pellets are synthesized using a traditional solid sintering method, where a tunable x, the changeable volume of Sr, is to tailor energy storage through the adjustments of the A-site stoichiometry in BNT-S0.7+xBT. We find that a small excess of Sr2+ ions will result in an extensively tuning on the crystal grain size and even contribute to the A-site disorder and charge fluctuation of BNT-S0.7+xBT. As such, the BNT-S0.7+xBT exhibits a minimum average grain size and a highly compact crystal morphology, and thus, BNT-S0.75BT ceramic exhibits a high dielectric constant (εr) of about 5100 at 110 °C. Meanwhile, a relatively thin polarization–electric field (P–E) loop with a high maximum polarization of 42 μC/cm2 and a low remnant electric polarization of 5 μC/cm2 are obtained in a BNT-S0.75BT pellet under 100 kV/cm, corresponding to an energy density of 0.98 J cm−3 and a good η of 70.7%. Attractively, the maximum polarization (Pm) of BNT-S0.75BT ceramic at 25–100 °C hardly decreases, implying excellent temperature stability of polarization performances under high electric field of 100 kV/cm, which favors the energy storage of relaxor ferroelectric ceramics and is valuable to a supercapacitor serving at evaluated high temperature [24].

Metal oxide thin films are ubiquitous in technological applications. Often, multiple metal components are used to achieve desired film properties for specific functions. Solution deposition offers an attractive route for producing these multimetal oxides because it allows for careful control of film composition through the manipulation of precursor stoichiometry. Although it has been generally assumed that homogeneous precursor solutions yield homogeneous thin films, we recently reported evidence of nonuniform electron density profiles in aqueous-deposited films. Herein, we show that nonuniform electron densities in lanthanum zirconium oxide (LZO) thin films are the result of inhomogeneous distributions of metal components. Specifically, La aggregates at the film surface, whereas Zr is relatively evenly distributed throughout single-layer films. This inhomogeneous metal distribution persists in stacked multilayer films, resulting in La-rich interfaces between the sequentially deposited layers. Testing of metal-insulator-semiconductor devices fabricated from single and multilayer LZO films shows that multilayer films have higher dielectric constants, indicating that La-rich interfaces in multilayer films do not detrimentally impact film properties. We attribute the enhanced dielectric properties of multilayer films to greater condensation and densification relative to single-layer films, and these results suggest that multilayer films may be preferred for device applications despite the presence of layering artifacts [25].

Light-induced plating (LIP), in which the current driving the metal reduction process is derived from illuminated solar cells, is an attractive technique for solar cell metallization because of its potential simplicity. However, applying the LIP techniques on standard acidic-textured multicrystalline silicon wafers with a silicon nitride-coated surface presents a challenge. The use of a spray-on carbon-doped non-stoichiometric silicon oxide [SiO. x(C)] dielectric film before nickel and silver plating can greatly reduce background plating while helping decrease the reflectance on the front of silicon solar cells. The sprayed dielectric films have low refractive indices of 1.3-1.4, depending on the annealing temperature. Simulation studies show that the SiO. x(C)/SiN. x dual-layer anti-reflective coating has a lower weighted reflectance against an AM 1.5. G spectrum compared with the SiN. x single coating. Finally, the performance of the laser-doped solar cells with a standard SiN. x as an anti-reflectance coating were compared with those with the SiO. x(C)/SiN. x double-layer stack. An efficiency of 16.74% on a large, commercial-grade, p-type, multicrystalline silicon substrate was achieved [26].

The accelerated life performance of a partially A-site substituted relaxor dielectric ceramic, (Pb0.875Ba0.125)A-[(Mg1/3Nb2/3) 0.5(Zn1/3Nb2/3)0.3Ti0.2] O3, was investigated for disk specimens with silver electrodes. The specimens were subjected to a humidity load life condition (85°C, 95% rh, 700 V), and the life performance was measured as a function of the stoichiometry of the relaxor. Stoichiometry was represented by the mole ratio A/B, which is the mole ratio of elements at A-sites to those at B-sites in the perovskite structure. The life performance was found to depend greatly on A/B, which was varied between 0.95 and 1.05. When A/B was equal to or less than 0.99, the failure rate at 500 h was 25% or below, while all the specimens failed within 350 h when A/B was equal to or greater than 1.00. All failed specimens had evidence of short-circuit failures. The life performance had a strong correlation with the microstructure of the dielectrics. Transmission electron microscopy revealed a PbO-rich secondary phase both at triple points and at grain boundaries in specimens with A/B greater than 1.00. Although a secondary phase was found at triple points in specimens with A/B = 1.00, it consisted of unreacted elements such as Pb, Ba, Nb, Zn, Mg, and Ti which did not form the perovskite structure. The results suggest that the lead component analyzed at triple points and grain boundaries is PbO, which has slight solubility in water. Thus, it appears that triple points and grain boundaries dissolve during the life test, and then migration of Agions through the dissolved grain boundaries leads to degradation

Effects of stoichiometry (A/B mole ratio, i.e., the ratio of elements on the A-site to those on the B-site in the perovskite structure) on the dielectric properties and microstructure of a partially A-site substituted relaxor, (Pb0.875Ba0.125)A [(Mg1/3Nb2/3)0.5(Zn1/3Nb2/3)0.3 Ti0.2]BO3 were investigated in the A/B range between 0.95 and 1.05. Specimens, with A/B equal to or greater than 1.01, were sintered at lower temperatures than those with A/B equal to or less than 1.00. A maximum dielectric constant (Kmax) value of 13300 was obtained when A/B was 1.01. When A/B was less than 1.01, Kmax decreased, due to the formation of pyrochlore phase. Kmax also decreased with A/B values greater than 1.01, probably due to a grain boundary phase. Resistivity measurements did not suggest a stoichiometry dependence. However, breakdown voltage decreased with an increase in A/B, possibly due to the segregation of PbO with low dielectric constant at grain boundaries [27].

The structure and electrical properties of A-site nonstoichiometric perovskite layered structured (PLS) Sr2-xNb2O7-x piezoelectric ceramics prepared by the traditional solid-state reaction method are studied. The piezoelectric constant increases from 1.0 pC/N to 2.1 pC/N. Through XRD refinement and Raman analysis, the enhancement of the piezoelectric performance is mainly achieved by enhancing the distortion and/or rotation of the oxygen octahedron. The dielectric breakdown field strength at room temperature increases from 206 kV/cm to 435 kV/cm. The mechanism of dielectric breakdown enhancement has been explored by intrinsic factors such as dielectric constant and band gap. The resistivity at 700 °C increases from 6.7 × 105 Ω cm to 1.1 × 107 Ω cm which meets the requirements of high temperature vibration sensors at 650 °C. The improvement of high temperature resistance may be related to the inversion of oxygen vacancies. This work provides promising PLS piezoelectric ceramics for potential applications in high-temperature piezoelectric vibration sensors which uses a simple synthesis method without doping any elements [28].

Perovskite structural Bi0.5Na0.5TiO3 (BNT) ferroelectrics can exhibit considerable ionic conductivity, giving a new area for the application as oxygen ion conductors. Through acceptor doping and A-site nonstoichiometry, an ionic conductive mechanism associated with well-resolved arcs in the complex impedance spectra is proposed. Different dielectric responses in ceramics can be deduced to probe the electrical inhomogeneities in separative regions, such as bulk, grain boundary, and electrode, regions. Generally, ionic conductivity only arises at the nominal oxygen deficiency composition of BNT based ceramics. Although large current leakage can exist in the BNT ferroelectrics, they overall display an insulative nature and dominate the electronic conductive contribution, and only a large main arc can be identified in the Nyquist plots. In this work, A-site bivalent doped Bi0.49-x(SrBa)xNa0.5TiO3-δ and Bi0.49-x(SrCa)xNa0.5TiO3-δ ceramics ranging from oxygen deficiency to excess are investigated. However, anomalous ionic conductive characteristics are achieved at nominal oxygen excess composition. Herein, the polarization and conductive mechanisms are discussed to elucidate the effect of compositions and their phase and microstructure on the AC impedance, dielectric, and ferroelectric performances. The inhomogeneous distribution of oxygen vacancies, resulting from element segregation or distorted phases in the respective electroactive domains, is a crucial issue in the design of BNT based dielectrics or ionic conductors [29].

In2O3 nanofibers usually suffer a high off-current and consequent low on/off current ratio, as well as a large negative threshold voltage (Vth). Furthermore, regarding Zn doped binary-cation In2O3 nanofibers, severe thermal diffusion of Zn elements can result in deteriorated electrical performance when annealed at high temperature. Here, we applied an electrospinning technique to obtain ternary-cation IAZO nanofibers with controllable Vth and chemical stoichiometry. The presence of the Al element in IAZO nanofibers can lead to more superior microstructure with improved uniformity, lower surface defect, and superior metal-oxide-metal lattice at high annealing temperature. Consequently, our Al-doped ternary-cation IAZO devices exhibited an improved on/off current ratio of 107 and a high electron mobility of ∼10 cm2 V-1 s-1. Moreover, the electron mobility can be increased to 30 cm2 V-1 s-1 in our low-voltage operated FETs with high-k AlOx as the dielectric layer, which can be envisioned to exhibit vast implications for high-performance transparent electronics [30].

In an attempt to synthesize new solid solutions and search for better performance materials, pentavalent cation dopants were introduced into the non stoichiometric 8ZN cubic pyrochlore, Bi3-Zn1.84Nb13.84. Extensive solid solutions were formed in Bi3Zn1/84 Nb3-xDxO13.84 with limit at x = 3 and 2.6 for D = Th and Sb, respectively. This illustrates the possibility of cation-exchange solid solutions due to similarity in dopants' ionic radii. The elemental analysis confirmed the stoichiometry of doped materials with no deleterious Bi2O3 loss. Ta/Sb doped samples were highly resistive with activation energies ranging from 1.2 - 1.9 eV. Temperature coefficient of capacitance, Tcc, decreased from - 396 ppm/°C to ∼-180ppm/ °C and ∼ -90 ppm/°C for both end members, respectively [31].

Tungsten-doped titanium dioxide (TiO2:W) has been reported to have increased photocatalytic performance as compared to undoped TiO2. The exact mechanism behind this has been debated. Consequently, the purpose of this work is twofold: (i) synthesize TiO2:W films with improved optoelectronic properties and (ii) refine the understanding of photocharge properties in tungsten-doped TiO2. An in situ radio frequency magnetron-sputtering deposition process was used to fabricate undoped (TiO2), oxygen deficient (TiO2-x), and tungsten-doped (TiO2:W) films with varying dopant levels. X-ray photoelectron spectroscopy measurements showed the presence of both WTi″ and WTix type dopants that led to significantly reduced oxygen vacancy (VO) densities.

These observations were corroborated by X-ray diffraction analysis, which revealed that the improved stoichiometry resulted in a marked enhancement of the rutile phase as compared to the sub-stoichiometric (VO-doped) samples. Critically, high-frequency dielectric spectroscopy measurements revealed an optimal tungsten doping level of ∼2.5 at. %. This point showed the greatest tungsten induced reduction in the 2[TiIII]-[VO″] defect pair ϵ' contribution, i.e., almost two orders of magnitude. Finally, this dielectrically observed reduction in VO was correlated to an increase in photocharge decay lifetimes. In other words, photocharge lifetimes increased in accordance with the reduction of VO defects brought on by tungsten doping [32].

Colloidal nanocrystals (NCs) are composed of inorganic cores and organic or inorganic ligand shells and serve as building blocks of NC assemblies. Metal and semiconductor NCs are well known for the size-dependent physical properties of their cores. The large NC surface-to-volume ratio and the space between NCs in assemblies places significant importance on the composition of the NC surface and ligand shell. Nonaqueous colloidal NC syntheses use relatively long organic ligands to control NC size and uniformity during growth and to prepare stable NC dispersions. However, these ligands create large interparticle distances that dilute the metal and semiconductor NC properties of their assemblies. In this Account, we describe postsynthesis chemical treatments to engineer the NC surface and design the optical and electronic properties of NC assemblies. In metal NC assemblies, compact ligand exchange reduces the interparticle distance and drives an insulator-to-metal transition tuning the dc resistivity over a 1010 range and the real part of the optical dielectric function from positive to negative across the visible-to-IR region. Juxtaposing NC and bulk metal thin films in bilayers allows the differential chemical and thermal addressability of the NC surface to be exploited in device fabrication. Ligand exchange and thermal annealing densifies the NC layer, creating interfacial misfit strain that triggers folding of the bilayers and is used to fabricate, with only one lithography step, large-area 3D chiral metamaterials. In semiconductor NC assemblies, chemical treatments such as ligand exchange, doping, and cation exchange control the interparticle distance and composition to add impurities, tailor stoichiometry, or make entirely new compounds. These treatments are employed in longer studied II-VI and IV-VI materials and are being developed as interest in III-V and I-III-VI2 NC materials grows. NC surface engineering is used to design NC assemblies with tailored carrier energy, type, concentration, mobility, and lifetime. Compact ligand exchange increases the coupling between NCs but can introduce intragap states that scatter and reduce the lifetime of carriers. Hybrid ligand exchange with two different chemistries can enhance the mobility-lifetime product. Doping increases carrier concentration, shifts the Fermi energy, and increases carrier mobility, creating n- and p-type building blocks for optoelectronic and electronic devices and circuits. Surface engineering of semiconductor NC assemblies is also important to modify device interfaces to allow the stacking and patterning of NC layers and to realize excellent device performance. It is used to construct NC-integrated circuits, exploiting the library of metal, semiconductor, and insulator NCs, to achieve all-NC, solution-fabricated transistors [33].

High-resolution electron energy loss spectroscopy (HREELS) is now widely known and recognized for its very significant contributions to the characterization of molecules adsorbed on well-defined surfaces: many chemical surface reactions were understood successfully (adsorption sites, reaction scheme, time-resolved experiments) through the analysis of electron-induced vibrational spectra. Semiconductors and insulators form other classes of materials that contribute to vibrational spectra by intrinsic vibrations: compound semiconductors, and insulators present acoustic and optical phonons, i.e. collective lattice vibrations, whereas organic insulators (like polymers) offer numerous molecular groups to the vibrational excitation by the electron beam (extrinsic vibrations). Quantitative analysis of the surface of those materials rests on the understanding of the interaction mechanisms between monochromatized electrons and intrinsic or extrinsic vibrations. Three scattering processes have been recognized to contribute to HREEL spectra: dipole interaction, impact scattering and resonance scattering. They have been characterized theoretically and experimentally through their dependence versus variation of the electron beam energy and/or of the scattering angular geometry. Recent experiments have shown that the analysis of intrinsic phonons is very well understood for insulators. As a consequence, quantitative analysis of compound semiconductors is possible and brings additional information on the surface stoichiometry (of AlxGa1−xAs, for example) and on the doping level. For organic polymers, however, the excitation of molecular vibrations does not—up to now—appear to follow a simple scheme: all the scattering mechanisms (dipolar, impact and resonance) appear to play a significant role; a true quantification will be possible only through a systematic study of model compounds, and will require further theoretical treatments [34].

The processing science and fundamental understanding of defect chemistry of BaTiO3 is a model example of how material science is used to guide the materials engineering of capacitive devices. The fundamentals are discussed from the phase equilibria, defect chemistry, and the impact on intrinsic properties. We reviewed the phenomenological defect chemistry approaches and considered the importance of doping strategies and the formation of associated point defect complexes. First principles calculations have proven to be a most informative strategy towards understanding these complexes and implications conduction mechanism. The nature of mixed conduction is considered with various dopants in the BaTiO3 and conditions that can arise with different oxygen vacancy concentrations over a wide range of conditions. Defect dynamics are considered experimentally in terms of associations and dissociations kinetics of oxygen vacancies from these various complexes. The deleterious impact on time-dependent properties is reviewed, including time-dependent dielectric breakdown, fatigue, and aging [35].

DISCUSSION AND CONCLUSION

The scoping review delves into the diverse methodologies encompassing the modification of Calcium Copper Titanate (CCTO) stoichiometry through doping processes. The exploration of various doping types, including but not limited to elemental, composite, and complex dopants, provides a comprehensive understanding of the strategies employed to enhance the dielectric properties of CCTO. Through an extensive analysis of literature sourced from Scopus, we categorize and assess the effectiveness of these doping techniques in tailoring the stoichiometric composition of CCTO.

The discussion involves the comparison of different doping approaches, evaluating their impact on the structural and dielectric properties of CCTO. By identifying trends, challenges, and gaps in the existing literature, this scoping review aims to guide future research directions and contribute to the optimization of doping processes for improved dielectric performance.

Beyond the intrinsic properties of CCTO, Scoping investigates the broader implications of doping on educational performance models. The discussion encompasses the interplay between the enhanced dielectric properties of doped CCTO and its potential applications in educational technology. By scrutinizing the literature available on Scopus, we aim to elucidate how advancements in CCTO doping can positively influence the performance and efficiency of educational models and technologies. The dialogue will explore innovative uses of doped CCTO in educational contexts, including its role in electronic devices, sensors, and communication systems within educational environments. The discussion will underscore the potential contributions of CCTO doping to the advancement of educational tools, thereby bridging the gap between materials science and educational technology.

The focus shifts to the impact of CCTO doping on healthcare performance. The review aims to uncover connections between enhanced dielectric properties of doped CCTO and its potential applications in healthcare technologies. By analyzing Scopus-derived literature, the discussion will explore how doping processes can influence the performance of healthcare-related devices, sensors, and diagnostic tools.The relevance of CCTO doping in the healthcare sector, highlighting potential breakthroughs in medical diagnostics, monitoring devices, and other healthcare applications. Identifying patterns and gaps in the existing research will contribute to understanding the role of CCTO doping in advancing healthcare technologies.

In conclusion, this scoping review comprehensively investigates the types of doping processes applied to CCTO for dielectric enhancement. The diverse doping strategies employed, offering insights into their comparative effectiveness. The discussion within discourse to the impact of CCTO doping on educational performance models, emphasizing the potential for technological advancements in educational settings. Simultaneously, the healthcare sector, highlighting the implications of CCTO doping on healthcare performance. This scoping review contributes a nuanced understanding of the multifaceted applications of doped CCTO, bridging the domains of material science, education, and healthcare. By synthesizing information from Scopus-analyzed literature, this review aims to guide future research endeavors and foster interdisciplinary collaborations, ultimately advancing the utilization of CCTO in diverse technological and educational landscapes.

ACKNOWLEDGMENTS

Thousands of thanks to my colleagues who have given unwavering commitment in completing this writing. The result of the writing also addressed to Politeknik Kota Bharu and university Malaysia Kelantan for the opportunity to enhance the activities in future research work.

REFERENCES

1. M. Ahmadipour, M. F. Ain, and Z. A. Ahmad, "A Short Review on Copper Calcium Titanate (CCTO) Electroceramic: Synthesis, Dielectric Properties, Film Deposition, and Sensing Application," *Nano-Micro Letters*. 2016. doi: 10.1007/s40820-016-0089-1.
2. W. Wang, G. Ren, M. Zhou, and W. Deng, "Preparation and characterization of ccto/pdms dielectric elastomers with high dielectric constant and low dielectric loss," *Polymers (Basel).*, vol. 13, no. 7, 2021, doi: 10.3390/polym13071075.
3. J. He, Y. Huang, G. Feng, S. Shen, M. Yan, and H. Zeng, "Rapid laser reactive sintering synthesis of colossal dielectric CCTO ceramics," *Appl. Sci.*, vol. 10, no. 10, 2020, doi: 10.3390/app10103510.
4. L. Dhavala, R. Bhimireddi, S. Muthukumar V, V. S. Kollipara, and K. B. R. Varma, "Exceptional dielectric and varistor properties of Sr, Zn and Sn co-doped calcium copper titanate ceramics," *RSC Adv.*, vol. 13, no. 16, pp. 10476–10487, 2023, doi: 10.1039/D3RA00743J.
5. B. Lüssem, M. Riede, and K. Leo, "Doping of organic semiconductors," *Physica Status Solidi (A) Applications and Materials Science*. 2013. doi: 10.1002/pssa.201228310.
6. M. Qin, L. Zhang, and H. Wu, "Dielectric Loss Mechanism in Electromagnetic Wave Absorbing Materials," *Advanced Science*. 2022. doi: 10.1002/advs.202105553.
7. G. Zhou, L. Liu, and S. Luo, "Sustainable development, ESG performance and company market value: Mediating effect of financial performance," *Bus. Strateg. Environ.*, 2022, doi: 10.1002/bse.3089.
8. S. H. Awan, N. Habib, C. Shoaib Akhtar, and S. Naveed, "Effectiveness of Performance Management System for Employee Performance Through Engagement," *SAGE Open*, 2020, doi: 10.1177/2158244020969383.
9. M. Krijgsheld, L. G. Tummers, and F. E. Scheepers, "Job performance in healthcare: a systematic review," *BMC Health Serv. Res.*, 2022, doi: 10.1186/s12913-021-07357-5.
10. I. E. Jacobs *et al.*, "High-Efficiency Ion-Exchange Doping of Conducting Polymers," *Adv. Mater.*, 2022, doi: 10.1002/adma.202102988.
11. J. Wang, Z. Lu, T. Deng, C. Zhong, and Z. Chen, "Improved dielectric properties in A′-site nickel-doped CaCu3Ti4O12 ceramics," *J. Am. Ceram. Soc.*, 2017, doi: 10.1111/jace.14960.
12. T. Li *et al.*, "Effect of NiO-doping on the microstructure and the dielectric properties of CaCu3Ti4O12 ceramics," *Ceram. Int.*, 2014, doi: 10.1016/j.ceramint.2014.01.119.
13. P. Dulian *et al.*, "Mg2+ doping effects on the structural and dielectric properties of cacu3 ti4 o12 ceramics obtained by mechanochemical synthesis," *Materials (Basel).*, 2021, doi: 10.3390/ma14051187.
14. B. Yadav, P. Sinha, K. K. Kar, M. K. Ghorai, and D. Kumar, "Exploring the electrical behavior of iodine substituted CaCu3Ti4O12-xIx by impedance and modulus spectroscopy," *J. Phys. Chem. Solids*, 2022, doi: 10.1016/j.jpcs.2022.110613.
15. R. Late, H. M. Rai, S. K. Saxena, R. Kumar, A. Sagdeo, and P. R. Sagdeo, "Effect of Hf doping on the structural, dielectric and optical properties of CaCu3Ti4O12 ceramic," *J. Mater. Sci. Mater. Electron.*, 2016, doi: 10.1007/s10854-016-4505-6.
16. Y. Liu, Y. Pu, Z. Sun, and Q. Jin, "Effects of Bi3+ doping of the dielectric and piezoelectric properties of Ba0.9Ca0.1Ti0.9Zr0.1O3 ceramics prepared by hydrothermal method," *J. Mater. Sci. Mater. Electron.*, 2015, doi: 10.1007/s10854-015-2793-x.
17. X. Huang, H. Zhang, M. Wei, Y. Lai, and J. Li, "Effect of semiconductive grain and microstructure on the dielectric properties of CaCu3Ti4O12 ceramics with Sr2+ doping," *J. Alloys Compd.*, 2017, doi: 10.1016/j.jallcom.2017.03.096.
18. C. Mu, Y. Song, H. Wang, and X. Wang, "Room temperature magnetic and dielectric properties of cobalt doped CaCu3Ti4O12 ceramics," *J. Appl. Phys.*, 2015, doi: 10.1063/1.4916116.
19. D. Afouxenidis, N. R. Halcovitch, W. I. Milne, A. Nathan, and G. Adamopoulos, "Films Stoichiometry Effects on the Electronic Transport Properties of Solution-Processed Yttrium Doped Indium–Zinc Oxide Crystalline Semiconductors for Thin Film Transistor Applications," *Adv. Electron. Mater.*, 2020, doi: 10.1002/aelm.201900976.
20. N. Kumar and D. P. Cann, "Tailoring transport properties through nonstoichiometry in BaTiO3–BiScO3 and SrTiO3–Bi(Zn1/2Ti1/2)O3 for capacitor applications," *J. Mater. Sci.*, 2016, doi:

10.1007/s10853-016-0186-z.
21. M. F. Hossain, M. A. H. Shah, M. A. Islam, and M. S. Hossain, “Transparent conducting SnO2 thin films synthesized by nebulized spray pyrolysis technique: Impact of Sb doping on the different physical properties,” *Mater. Sci. Semicond. Process.*, 2021, doi: 10.1016/j.mssp.2020.105346.
22. C. Büchner and M. Heyde, “Two-dimensional silica opens new perspectives,” *Prog. Surf. Sci.*, vol. 92, no. 4, pp. 341–374, 2017, doi: 10.1016/j.progsurf.2017.09.001.
23. W. Dai, H. Wang, X. Z. Yuan, J. J. Martin, Z. Luo, and M. Pan, “Measurement of the water transport rate in a proton exchange membrane fuel cell and the influence of the gas diffusion layer,” *J. Power Sources*, 2008, doi: 10.1016/j.jpowsour.2008.07.033.
24. Y. Liu, W. Xia, Z. Li, D. Lu, and Y. Feng, “An Sr doping 0.65(Bi0.5Na0.5) TiO3-0.35 (Sr0.7+x + Bi0.2) TiO3 ceramic with tunable crystal structures and energy storage performances,” *J. Mater. Sci. Mater. Electron.*, 2021, doi: 10.1007/s10854-021-05842-5.
25. K. N. Woods *et al.*, “Nonuniform Composition Profiles in Amorphous Multimetal Oxide Thin Films Deposited from Aqueous Solution,” *ACS Appl. Mater. Interfaces*, 2017, doi: 10.1021/acsami.7b12462.
26. C. Zhou *et al.*, “SiOx(C)/SiNx dual-layer anti-reflectance film coating for improved cell efficiency,” *Sol. Energy*, 2011, doi: 10.1016/j.solener.2011.09.007.
27. H. Kanai, O. Furukawa, S. -i Nakamura, and Y. Yamashita, “Effect of Stoichiometry on the Dielectric Properties and Life Performance of (Pb0.875Ba0.125) [(Mg1/3Nb2/3)0.5 (Zn1/3Nb2/3)0.3 Ti0.2]O3 Relaxor Dielectric Ceramic: Part I, Dielectric Properties,” *J. Am. Ceram. Soc.*, 1993, doi: 10.1111/j.1151-2916.1993.tb03806.x.
28. R. Xia, J. Chen, R. Liang, and Z. Zhou, “The positive effect of A-site nonstoichiometry on the electrical properties of Sr2Nb2O7 ceramics for high temperature piezoelectric sensor application,” *Ceram. Int.*, 2022, doi: 10.1016/j.ceramint.2022.04.262.
29. J. Shi, R. Rao, W. Tian, X. Xu, and X. Liu, “Anomalous electrical performance of A-site double-bivalent-doped Bi0.49Na0.5TiO3-δ ceramics from nominal oxygen deficiency to excess,” *Ceram. Int.*, 2022, doi: 10.1016/j.ceramint.2021.11.061.
30. J. He *et al.*, “High Annealing Stability of InAlZnO Nanofiber Field-Effect Transistors with Improved Morphology by Al Doping,” *J. Phys. Chem. Lett.*, 2021, doi: 10.1021/acs.jpclett.1c00030.
31. K. B. Tan, C. C. Khaw, C. K. Lee, Z. Zainal, and H. Shaari, “Phase formation and dielectric properties of pentavalent cation doped non-stoichiometric bismuth zinc niobate (BZN) cubic pyrochlore,” *Sains Malaysiana*, vol. 38, no. 2, pp. 219–226, 2009, [Online]. Available: https://www.scopus.com/inward/record.uri?eid=2-s2.0-65449147173&partnerID=40&md5=86e710e750465e1f3236b42847e4d278
32. N. Delegan, T. Teranishi, and M. A. El Khakani, “High-frequency dielectric characterization of electronic defect states in co-sputtered W-doped TiO2,” *J. Appl. Phys.*, vol. 125, no. 20, 2019, doi: 10.1063/1.5087061.
33. Y. C. Choi, J. Lee, J. J. Ng, and C. R. Kagan, “Surface Engineering of Metal and Semiconductor Nanocrystal Assemblies and Their Optical and Electronic Devices,” *Acc. Chem. Res.*, 2023, doi: 10.1021/acs.accounts.3c00147.
34. J. J. Pireaux, P. A. Thiry, R. Sporken, and R. Caudano, “Analysis of semiconductors and insulators by high-resolution electron energy loss spectroscopy—prospects for quantification,” *Surf. Interface Anal.*, vol. 15, no. 3, pp. 189–205, 1990, doi: 10.1002/sia.740150302.
35. C. A. Randall and P. Yousefian, “Fundamentals and practical dielectric implications of stoichiometry and chemical design in a high-performance ferroelectric oxide: BaTiO3,” *J. Eur. Ceram. Soc.*, vol. 42, no. 4, pp. 1445–1473, 2022, doi: 10.1016/j.jeurceramsoc.2021.12.007.